

**Biomass-based Composites from Poly(lactic acid) and Wood Flour by Vapor Phase Assisted Surface Polymerization**

Donghee Kim,<sup>a</sup> Yoshito Andou,<sup>b</sup> Yoshihito Shirai,<sup>a,b</sup> Haruo Nishida<sup>b,\*</sup>

*<sup>a</sup>Graduate School of Life Science and Systems Engineering, Kyushu Institute of Technology, 2-4 Hibikino, Wakamatsu-ku, Kitakyushu, Fukuoka 808-0196, Japan*

*<sup>b</sup> Eco-Town Collaborative R&D Center for the Environment and Recycling, Kyushu Institute of Technology, 2-4 Hibikino, Wakamatsu-ku, Kitakyushu, Fukuoka 808-0196, Japan*

**Corresponding author:** Haruo Nishida<sup>\*</sup>

<sup>\*</sup> Tel/Fax +81-93-695-6233 E-mail address: nishida@lsse.kyutech.ac.jp

**Running Head:**

Biomass-based Composites from PLLA and Wood Flour by VASP

**Abstract**

In order to prepare biomass-based composites in an environmentally benign manner, vapor phase-assisted surface polymerization (VASP) was applied to prepare the composites from wood flour and poly(L-lactic acid) (PLLA) without solvent. VASP of L-lactic acid (LLA) successfully proceeded on the wood flour surfaces and newly generated PLLA, which had very high crystallinity, covered up the wood flour surfaces. Obtained PLLA/wood flour composites were clarified that the grafting of PLLA on wood flour surfaces occurred to form covalently bonded composites, and the accumulated PLLA layers crystallized in situ during VASP. Resulting PLLA layers showed nearly complete crystallinity of 99.7% and a high melting point close to the equilibrium melting point. Moreover, thermal degradation behavior of the composites suggested a cooperative degradation manner of the components.

**Key Words**

biomass-based composites / wood flour / poly(L-lactic acid) / vapor phase-assisted surface polymerization

## INTRODUCTION

Lignocellulosic materials such as wood flour are abundant renewable resources. The materials include versatile cellulose fibers as a main component. Many researchers have investigated composite materials composed of petroleum-based polymers and lignocellulosic materials, such as jute,<sup>[1,2]</sup> coconut,<sup>[3]</sup> sisal,<sup>[4]</sup> and kenaf<sup>[5]</sup> fibers to develop high-performance materials reinforced by the natural fibers.

Lately, many kinds of bio-based polymeric materials have been developing for uses as blend components because of their carbon neutral property and biodegradability. Poly(L-lactic acid) (PLLA) is a typical bio-based aliphatic polyester produced from starch, molasses, etc.<sup>[6]</sup> via lactic acid fermentation, oligomerization, cyclic-dimerization, and ring-opening polymerization<sup>[7]</sup> of the cyclic dimer, lactide, or direct polycondensation of lactic acid.<sup>[8,9,10,11]</sup> PLLA has some good physical properties such as transparency, high elastic modulus, high melting temperature around 170°C,<sup>[12]</sup> etc. PLLA could be applied in various fields such as medical devices,<sup>[13]</sup> composite materials,<sup>[14,15,16,17,18,19]</sup> and packages.<sup>[20]</sup>

Composites made from natural fibers and PLLA matrices<sup>[21]</sup> have been investigated as promised materials having low environmental impact in comparison with petroleum-based polymer composites. When natural materials are incorporated into commodity plastic matrices, it has been shown to weaken the mechanical properties of composites because of the poor interfacial interactions between the hydrophobic matrices and the hydrophilic fillers,<sup>[22]</sup> which have a large number of hydroxyl and/or carboxyl groups on surfaces.

Surface modification is an important method to improve the interfacial adhesion between natural fibers and hydrophobic matrices. Many efforts have been made for this subject, for example, by using silane-crosslinking for wood/PE,<sup>[ 23 , 24 , 25 ]</sup> esterification-branching/crosslinking for wood/PE/PP<sup>[26]</sup> and wood/PLA,<sup>[27]</sup> etc.

The vapor-phase assisted surface polymerization (VASP) technique has been developed to coat various substrate surfaces by polymers without any solvent,<sup>[28,29,30,31,32,33,34]</sup> resulting in achievements of block-copolymer coating, surface grafting, hydrophobic/hydrophilic control, and micropatterning on the surfaces. During the VASP processes, vaporized monomers can diffuse and penetrate into internal gaps and spaces of solid substrates, even if nano-spaces between silicate layers of montmorillonite to exfoliate them by in-situ VASP.<sup>[35,36]</sup> VASP is also an excellent method to keep fine structures of delicate substrate surfaces such as biomaterials, while to modify their chemical properties, because the processes: adsorption of gaseous monomer molecules and simultaneous polymerization are very gentle in comparison with convenient liquid and melt processes.<sup>[37]</sup> Moreover, there are two additional properties of VASP: an interfacial interaction with substrate surfaces and formation of highly crystallized polymer layers.<sup>38</sup> These properties suggest constructions of specific composites with various properties different with previously reported

composites prepared by the liquid and melt processes.

In this study, VASP of L,L-lactide was carried out on surfaces of wood flour to produce a biocompatible composite, which is expected to show specific properties based on the simultaneous polymerization/crystallization processes of PLLA. To clarify the structure and properties of PLLA/wood flour composites, obtained composites were examined by various analytical methods.

## EXPERIMENTAL

### Materials

Monomer: L,L-lactide (LLA, 99.6%, melting point 97°C) was purchased from Musashino Co., Ltd. (Tokyo, Japan) and purified by two times recrystallization from toluene before use. Substrate: wood flour of Japanese cedar (average diameter: 500  $\mu\text{m}$ ) was purchased from TRYWOOD Co., Ltd. (Hita, Japan) and used as received. Catalyst, Sn(II) 2-ethylhexanoate ( $\text{Sn}(\text{Oct})_2$ ) was purchased from Wako Pure Chemical Industries, Ltd. (Wako, Japan) and used as received. Commercialized poly(L-lactic acid) (PLLA) ( $M_n$  xxxxxx,  $M_w$  xxxxxx) received from xxxxxxxxx was used as a reference material: pure PLLA. All the solvents were commercially obtained and used as received.

### Typical procedure of VASP

Substrate: wood flour (2.0 g) was pre-treated with a 0.25 mM  $\text{CH}_2\text{Cl}_2$  solution of  $\text{Sn}(\text{Oct})_2$  (50 mL) at a weight ratio of wood flour:  $\text{Sn}(\text{Oct})_2 = 20:1$  (wt/wt) and 25°C for 0.5 h under stirring to adsorb the catalyst on the surface. After the pre-treatment,  $\text{CH}_2\text{Cl}_2$  was removed under vacuum at 20 °C, resulting in the preparation of catalyst-supported wood flour substrate.

A typical procedure of VASP was carried out in an H-shaped glass tube reactor with a vacuum cock. The catalyst-supported wood flour (200 mg) was put into a Petri dish (bottom surface area: 116.9  $\text{mm}^2$ ) and the Petri dish was set in the bottom of one of the legs of the H-shaped glass tube reactor. Monomer: LLA (2.5g, 17.5 mmol) was introduced into the bottom of the other leg. The reactor was degassed by three freeze-pump-thaw cycles and then sealed under a saturated atmosphere of vaporized LLA. Polymerization was carried out at 110 °C for 24 h in a thermostated oven. At the temperature, LLA was melted and evaporated to show a saturated vapor pressure ( $1.25 \times 10^3$  Pa).

After VASP, obtained product was dried to remove the adsorbed LLA molecules *in vacuo* and weighed to yield 1.85 g of the PLLA/wood flour composite. The product was analyzed intact with Fourier transform infrared (FTIR) spectroscopy, scanning electron microscopy (SEM), thermogravimetry (TG), differential scanning calorimetry (DSC), and wide angle X-ray diffractometry (WAXD).

Free-polymers in the PLLA/wood flour composite were extracted by  $\text{CHCl}_3$  from the product with a Soxhlet apparatus for 24 h. The isolated polymers were dried and analyzed by FT-IR,

<sup>1</sup>H-NMR spectroscopy, and size-exclusion chromatography (SEC).

### Characterization

<sup>1</sup>H-NMR spectra were measured on a 500-MHz JEOL JNM-ECP500 FT-NMR spectrometer. Chloroform-*d* was used as a solvent and the chemical shifts were reported as  $\delta$  values (ppm) relative to internal tetramethylsilane (TMS) unless otherwise noted. FT-IR spectroscopy was performed using a Perkin Elmer GX2000R FTIR spectrometer equipped with an attenuated total reflectance (ATR) crystal accessory (Golden Gate). SEM observation was performed with a HITACHI S3000N scanning electron microscope at an accelerating voltage of 5.0 kV.

TG analyses were performed using a SEIKO EXSTAR 6200 TG/DTA system under nitrogen flow (100 mL·min<sup>-1</sup>) in a temperature range of 30-500 °C. About 6 mg of sample was placed in an aluminum pan and measured. DSC measurements were performed on an SEIKO EXSTAR 6200 DSC system in a nitrogen atmosphere. About 6 mg of the sample was placed on an aluminum pan and first scanned from room temperature up to 200°C by a heating rate of 10 °C·min<sup>-1</sup>, cooled to 20 °C by a cooling rate of 10 °C·min<sup>-1</sup>, and then second scanned by the same heating rate in a nitrogen flow of 50 mL·min<sup>-1</sup>.

WAXD patterns were measured on a Rigaku XRD-DSC-X II diffractometer using Cu-K $\alpha$  radiation ( $\lambda = 0.1541$  nm) at room temperature in a  $2\theta$  range of 10-40° at a scanning rate of 2 deg·min<sup>-1</sup>. Molecular weights of polymers were measured on a TOSOH HLC-8120 size exclusion chromatography (SEC) system with refractive index (RI) and ultraviolet (UV,  $\lambda = 254$  nm) detectors under the following conditions: TSKgel Super HM-H linear column (linearity range,  $1 \times 10^3 - 8 \times 10^6$ ; molecular weight exclusion limit,  $4 \times 10^8$ ), CHCl<sub>3</sub> (HPLC grade) eluent at a flow rate of 0.6 mL·min<sup>-1</sup>, and column temperature of 40 °C. Calibration curves for SEC analysis were obtained using polystyrene standards with a low polydispersity ( $7.70 \times 10^2$ ,  $2.43 \times 10^3$ ,  $3.68 \times 10^3$ ,  $1.32 \times 10^4$ ,  $1.87 \times 10^4$ ,  $2.93 \times 10^4$ ,  $4.40 \times 10^4$ ,  $1.14 \times 10^5$ ,  $2.12 \times 10^5$ ,  $3.82 \times 10^5$ ,  $5.61 \times 10^5$ ,  $2.00 \times 10^6$ , Aldrich). The sample (15 mg) was dissolved in chloroform (3 mL) and the solution was filtered through a membrane filter with 0.45  $\mu$ m pore size. The SEC traces were evaluated by a universal calibration method (UCM) using the published Mark-Houwink-Sakurada constants<sup>[39]</sup> for PLLA and polystyrene at 40 °C as follows: ”

$$\text{PLLA :} \quad [\eta] = (2.068 \times 10^{-4}) M^{0.734}$$

$$\text{Polystyrene :} \quad [\eta] = (2.072 \times 10^{-4}) M^{0.655}$$

## RESULTS AND DISCUSSION

### VASP of LLA on wood flour surfaces

Vapor-phase assisted surface polymerization (VASP) of L,L-lactide (LLA) was carried out on

wood flour as a substrate, on which surfaces Sn(II) 2-ethylhexanoate ( $\text{Sn}(\text{Oct})_2$ ) as a well-known catalyst for the anionic ring-opening polymerization of LLA was supported.<sup>[40]</sup> The polymerization was conducted under saturated vapor pressure ( $1.25 \times 10^3$  Pa) of LLA at 110 °C as listed in Table 1. Monomer molecules in the gaseous phase were once adsorbed on the surface and undergo the polymerization. Since the reaction temperature was set at a higher temperature by 13 °C than the melting point of LLA, the adsorbed LLA molecules can diffuse on the substrate surface to undergo the polymerization. During VASP, the substrate monotonously increased in weight and enlarged in volume with time (Table 1). After 24 h, the product was appeared as a lump of aggregated powdery solid (entry No. 5). Based on the amount of increase in weight, the product after 24h was estimated to be comprised the original wood flour of 13.2 wt% and the newly generated materials of 86.2 wt%. In Figure 1, FT-IR spectrum of the product No. 5 showed no peak in a wavenumber range of 3100–3700  $\text{cm}^{-1}$  corresponding to hydroxyl groups of wood flour, indicating that the surfaces were covered up by accumulated materials.

To confirm newly accumulated materials on the wood flour surfaces, the products in Table 1 were extracted using  $\text{CHCl}_3$  with a Soxhlet extraction apparatus. FT-IR spectrum of the extracted material in Figure 1 showed the same pattern as that of pure PLLA, exhibiting characteristic peaks of PLLA at 1760  $\text{cm}^{-1}$  assigned to  $\nu_{\text{C=O}}$  and 1194, 1130, and 1047  $\text{cm}^{-1}$  assigned to  $\nu_{\text{C-O}}$ .<sup>[41]</sup>

Table 1  
Figure 1 FTIR

Figure 2 shows the changes in SEC profile of the extracted materials from products in Table 1. From the analyses of the SEC profiles, the extracted materials were found to be polymeric materials having a low molecular weight range of  $M_w$  1,300 - 10,000 with a wide polydispersity index (PDI) value in a range of 2.5 - 4.0. In Figure 3,  $^1\text{H}$  NMR spectra of the extracted materials after 6 and 24 h of VASP (No. 2 and 5 in Table 1) are illustrated in comparison with pure PLLA. Observed sharp doublet at 1.57/1.59 ppm and quintet at 5.14-5.20 ppm were assigned to characteristic signals of  $-\text{CH}_3$  and  $>\text{CH}-$  in PLLA, respectively. Therefore, these results indicate that the newly accumulated polymeric materials on the wood flour surfaces were PLLA.

Figure 2 GPC  
Figure 3 NMR

All the SEC profiles in Figure 2 showed similar multi-modal shapes, reflecting the heterogeneity of VASP process on the wood flour surfaces in comparison with conventional liquid and bulk polymerization processes.<sup>[42]</sup> The multimodal shape shifted into higher molecular weight

regions with progress in the polymerization. In spite of the heterogeneity of VASP process, the polymer yield and molecular weight were monotonously increased in parallel with time (Table 1, Figure S1 and S2 in Supporting Information), accompanying decreases in polydispersity index (PDI) value. These results indicate that most polymer chains continue to grow during VASP without considerable termination reactions, suggesting a controlled polymerization manner similarly to previous results of VASP using  $\epsilon$ -propiolactone.<sup>[43]</sup>

#### *Changes in morphology of wood flour surfaces*

The substrate wood flour varied its morphology with the expanding in volume during VASP. The variations in the morphology of wood flour were examined by SEM observation. Figure 4 shows SEM images of the wood flour surfaces before (Figure 4a) and after VASP (Figure 4b). Obviously, the wood fibers increased in thickness and their surfaces became flat after VASP due to covering by accumulated PLLA layers. After the extraction treatment by  $\text{CHCl}_3$ , the fine structures of wood flour were recovered as shown in Figure 4c.

Figure 4 SEM images

#### *Determination of grafting from wood flour components*

In Figure 1, FT-IR spectra of composite and extracted PLLA exhibited the same characteristic peaks with pure PLLA at  $1760\text{ cm}^{-1}$  assignable to  $\nu_{\text{C=O}}$ . However, these carbonyl peaks appeared to be broadened with tailing in comparison with pure PLLA.<sup>[44]</sup> The wood flour components: hemicellulose and lignin show carbonyl peaks  $\nu_{\text{C=O}}$  at  $1735\text{ cm}^{-1}$ .<sup>[45,46]</sup> In Figure S3 in Supporting Information, a difference spectrum between the extracted sample No.5 and pure PLLA is illustrated in comparison with original wood flour. Characteristic peaks at  $1731\text{ cm}^{-1}$  and  $1020\text{ cm}^{-1}$  for  $\nu_{\text{C=O}}$  and  $\nu_{\text{C-O}}$ , respectively, suggesting the grafting of PLLA on hemicellulose and/or lignin chains.

The carbonyl peak of residual wood flour after the extraction treatment also appeared to be broad around  $1749\text{ cm}^{-1}$  different with the carbonyl peak at  $1735\text{ cm}^{-1}$  of original wood flour (Figure 1). The wood flour after the extraction treatment showed superior water repellency as well as the PLLA/wood flour composite. These characteristics indicate the grafting of PLLA chains on the wood flour surfaces.

Figure 5 shows changes in UV/RI intensity ratio of each fraction in SEC profiles of pure PLLA and the extracted sample No. 5 after VASP of 24 h. The UV/RI intensity ratio of homopolymers should be nearly constant.<sup>[47]</sup> Pure PLLA showed nearly constant UV/RI intensity ratio in a range of 0.03 – 0.04 over the whole peak profile (Figure 5a). On the other hand, the UV/RI intensity ratio of sample No.5 (Figure 5b) increased from 0.03 to 0.6 with increase in molecular weight of PLLA. If the PLLA chains graft on/from other materials having different UV/RI intensity

ratio values, measured UV/RI ratio value must vary with grafting efficiency, by which the solubility of graft copolymers in  $\text{CHCl}_3$  may be also varied. When the other materials for grafting were polymeric materials, the grafting of PLLA branch chains might occur at plural points on the stem chains, causing the increase in total molecular weight and its solubility. Figure 5b obviously showed the increase in the UV/RI ratio value in accordance with the increase in molecular weight of each fraction. This means that the higher the grafting efficiency was, the more the molecular weight and UV/RI ratio increased.

Other samples, No. 1-4 in Table 1 also exhibited similar tendencies in the UV/RI ratio value on their SEC profiles. Moreover, the total UV/RI ratio values over their whole peak profiles decreased with increase in the increment of PLLA accumulation, reflecting that a negative effect of the chain growth increment offsetted the effect of grafting (Table S1 in Supporting Information).

These results indicate that during VASP some wood flour components were incorporated into first-structures of the accumulated PLLA chains in various manners of covalently bonding such as the grafting.

Figure 5 SEC profile UV/RI ratio

#### *Thermal properties of wood flour/PLLA composites*

Thermogravimetric (TG) and differential TG (DTG) profiles of original wood-flour and PLLA/wood-flour composites are shown in Figure 6. All the samples showed multi-step degradation behaviors as reflecting each corresponding degradation step of components. Many minor DTG peaks at low temperatures reflect the heterogeneous initiation and propagation processes of VASP on the wood flour surfaces.<sup>[48]</sup>

The profile of original wood flour was consisted of two narrow temperature regions (250-320 and 320-375 °C) and a wide region (160-900 °C<sup>[49]</sup>) for degradation of hemicellulose, cellulose, and lignin components, respectively. The accumulation of PLLA layers on the surface by VASP added more complex degradation steps into the wood flour profile, and caused shifts of the wood flour degradation steps into low temperature ranges, suggesting an acceleration of the wood flour degradation by the accumulated PLLA.

Main DTG peaks of PLLA degradation clearly appeared and gradually shifted into higher temperature ranges with increase in molecular weight of the PLLA ingredient. This result means that the higher the molecular weight of accumulated PLLA is, the more stable the composite becomes. Moreover, the degradation temperature range of substrate was also recovered at nearly original range with the increase in molecular weight of PLLA.

Interestingly, when the accumulated PLLA layers were removed by the extraction treatment, the residual wood flour ingredient showed nearly the same TG curves with the original wood flour



(Figure S4 in Supporting Information). These cooperative degradation behaviors of the composites make us image that there are specific interactions at interfaces between the wood flour substrate surfaces and the accumulated PLLA layers.

Figure 6 TG profiles

#### *Crystallization behavior on wood flour surfaces*

Crystallization behaviors of accumulated PLLA layers during VASP were analyzed with WAXD. In Figure 7, WAXD profiles of original wood flour and products No. 1-5 in Table 1 are illustrated. The wood flour profile showed broad peaks at  $2\theta = 14.9, 16.3, 22.5,$  and  $34.6^\circ$  assigned to diffraction plains (101),  $(10\bar{1})$ , (002), and (040) of cellulose crystalline, respectively.<sup>[50]</sup> The diffractions from cellulose crystalline became covered up by the accumulated PLLA layers during VASP. The accumulated PLLA layers after 24 h of VASP smoothly crystallized to finally reach 99.7 % in crystallinity from the WAXD profile as shown in Figure 7. The WAXD profiles after 24h of VASP showed a typical diffraction pattern of the  $\pm$ -form crystalline of PLLA.<sup>[51,52]</sup> Two strongest diffraction peaks at  $2\theta = 16.6$  and  $19.0^\circ$  correspond to the diffractions of (110)/(200) and (203) plains, respectively.

Interestingly, the WAXD pattern of PLLA layers varied with time of VASP. After 3h, weak diffraction peaks at  $2\theta = 11$  and  $16.5^\circ$  were found, and after 9h other diffraction peaks at  $2\theta = 10.9, 14.8$  (010),  $16.45$  (110)/(200),  $18.8$  (203),  $20.0, 20.7$  (204),  $23.7$  (015),  $26.8$  (207),  $28.7$  (018), and  $307^\circ$  (1010) were appeared. As shown in an interposition of Figure 7, significant shifts of the diffraction peak positions from the plains (110)/(200) and (203) were observed from  $16.45$  to  $16.6^\circ$  and from  $18.8$  to  $19.0^\circ$  during VASP of 9h to 24h, respectively. These shifts attribute to decreases in lattice spaces of crystalline (Table S2 in Supporting Information), meaning that the crystalline structure of PLLA transformed from a disorder  $\pm\bullet$ -form to order  $\pm$ -form crystal.<sup>[53,54,55]</sup>

The progress in VASP caused not only the disorder-to-order ( $\pm\bullet$ -to- $\pm$ ) transition in PLLA crystalline, but also increase in the crystalline size as shown in Table S2, which increases were evaluated from the half-width values of diffraction peaks from the plains (110)/(200) and (203).

Above  $\pm\bullet$ -to- $\pm$  transition and nearly complete crystallinity of PLLA crystalline must be due to the polymerization temperature of  $110^\circ\text{C}$ , at which temperature PLLA crystalline causes the transition easily,<sup>[56]</sup> especially low molecular weight PLLAs show high crystal growth rates.<sup>[57]</sup> Assignments of newly found diffraction peaks at  $10.9$  and  $20.0^\circ$  are now in progress and will be reported elsewhere in a near future.

Figure 7 XRD

In order to confirm the high crystallinity of accumulated PLLA layers, melting point ( $T_m$ ) and enthalpy change in the melting ( $\Delta H_m$ ) of PLLA samples after VASP were measured by DSC. Figure 8 shows 1<sup>st</sup> and 2<sup>nd</sup> scanned DSC curves of PLLA/wood flour composite (sample No 5). At the 1<sup>st</sup> scan, the sample showed relatively high melting temperature  $T_m = 174.1^\circ\text{C}$  with a high  $\Delta H_m$  value of  $xx \text{ J}\cdot\text{g}^{-1}$ , and at following 2<sup>nd</sup> scan, the same sample showed low  $T_m = 165.6^\circ\text{C}$  with a high  $\Delta H_m$  value of  $xx \text{ J}\cdot\text{g}^{-1}$ . Pan et al.<sup>[58]</sup> reported  $T_m$  values of PLLAs having various molecular weights. In their report, a low molecular weight PLLA ( $M_n$  15,400,  $M_w$  21,300) exhibited a lower  $T_m = 160.9^\circ\text{C}$  than  $173.4^\circ\text{C}$  of a high molecular weight PLLA ( $M_n$  218,600,  $M_w$  359,200). In this study, in spite of lower molecular weights ( $M_n$  4,700,  $M_w$  12,100) of sample No. 5, the  $T_m$  value on 1<sup>st</sup> scan was higher than that of the high molecular weight PLLA, and, interestingly, nearly the same with the equilibrium  $T_m^0$  ( $174.2^\circ\text{C}$ ) of the low molecular weight PLLA ( $M_w$  12,100). After once melting, the 2<sup>nd</sup> scanned DSC curve of the sample No. 5 showed a low value of  $T_m = 165.6^\circ\text{C}$ , even though higher than that of the low molecular weight PLLA ( $M_w$  12,100).

Thus, the accumulated PLLA layers during VASP at  $110^\circ\text{C}$  were easily crystallized on the substrate surfaces to show a nearly equal to the equilibrium temperature of PLLA having a similar molecular weight. These results indicate that there are some interaction effects between the wood flour surfaces and PLLA layers, for example, the wood flour surfaces effectively accelerate the crystallization of PLLA layers accumulated on them.

Figure 8 DSC

## Conclusions

Vapor phase-assisted surface polymerization (VASP) was applied to prepare biomass-based composites from wood flour and PLLA. VASP of PLLA successfully proceeded on wood flour surfaces and newly generated PLLA, which had very high crystallinity, accumulated and covered up the surfaces. From FT-IR and SEC analyses of obtained PLLA/wood flour composites, it was clarified that the grafting of PLLA on wood flour surfaces proceeded to form covalently bonded composites. From WAXD and DSC analyses, the accumulated PLLA layers crystallized in situ during VASP at  $110^\circ\text{C}$ , resulting in very high crystallinity of 99.7% and high  $T_m$  close to the equilibrium  $T_m^0$ . These results demonstrate that there are some interaction effects between the wood flour surfaces and PLLA layers. Thermal degradation behavior of composites was also investigated and it was observed that the degradation proceeded in a cooperative manner of the ingredients, such as the acceleration of degradation by accumulated PLLA. From these results, it was determined that specific biomass-composites, in which the interfaces were effectively bonded with the highly crystallized PLLA coating, were achieved.

## References

- [1] N. Chand, U. K. Dwivedi, *Wear*. 2006, 261, 1057.
- [2] A. K.Rana, A. Mandal, S. Bandyopadhyay, *Compos. Sci. Technol*. 2003, 63, 801.
- [3] M.Brahmakumar, C. Pavithran, R. M. Pillai, *Compos. Sci. Technol*. 2005, 65, 563.
- [4] P. A. Sreekumar, K. Joseph, G. Unnikrishnan, S. Thomas, *Compos. Sci. Technol*. 2007, 67, 453.
- [5] M. Zampaloni, F. Pourboghrat, S. A. Yankovich, B. N. Rodgers, J. Moore, L. T. Drzal, A. K. Mohanty, M. Misra, *Compos., Part A: Appl S*. 2007, 38, 1569.
- [6] H. R. Kricheldorf, I. Kreiser-Saunders, C. Boettcher, *Polymer* 1995, 36, 1253.
- [7] A. Takasu, Y. Narukawa, T. Hirabayashi, *J. Polym. Sci. Pol. Chem*. 2006, 44, 5247. [8] K. W. Kim, S. I. Woo, *Macromol. Chem. Physic*. 2002, 203, 2245.
- [9] F. Achmad, K. Yamane, S. Quan, T. Kokugan, *Chem. Eng. J*. 2009, 151, 342.
- [10] G.-X.Chen, H.-S. Kim, E.-S. Kim, J.-S. Yoon, *Eur. Polym. J*. 2006, 42, 468.
- [11] P. Yin, N. Nishina, Y. Kosakai, K. Yahiro, Y. Pakr, M. Okabe, *J. Ferment. Bioeng*. 1997, 84, 249.
- [12] T. Kasuga, Y. Ota, M. Nogami, Y. Abe, *Biomaterials* 2001, 22, 19.
- [13] M. S. Huda, L. T. Drzal, A. K. Mohanty, M. Misra, *Compos. Sci. Technol*. 2006, 66, 1813.
- [14] F. Chen, L. S. Liu, P. H. Cooke, K. B. Hicks, J. W. Zhang, *Ind. Eng. Chem. Res*. 2008, 47, 8667.
- [15] T. Nishino, K. Hirao, M. Kotera, *Compos., Part A: Appl S*. 2006, 37, 2269.
- [16] T.-M. Wu, C.-Y. Wu, *Polym. Degrad. Stabil*. 2006, 91, 2198.
- [17] L. Petersson, I. Kvien, K. Oksman, *Compos. Sci. Technol*. 2007, 67, 2535.
- [18] M. Noël, E. Fredon, E. Mougél, D. Masson, E. Masson, L. Delmotte, *Bioresource Technol*. 2009, 100, 4711.
- [19] L. T. Lim, R. Auras, M. Rubino, *Prog. Polym. Sci*. 2008, 33, 820.
- [20] G. Grubbstrom, A. Holmgren, K. Oksman, *Compos., Part A: Appl S*. 2010, 41, 678.
- [21] M. Bengtsson, K. Oksman, *Compos., Sci. Technol*. 2006, 66, 2177.
- [22] M. Bengtsson, K. Oksman, *Compos., Part A: Appl S*. 2006, 37, 752.
- [23] S. Thiebaud, M. E. Borredon, *Bioresource Technol*. 1995, 52, 169.
- [24] C.-S. Wu, *Polym. Degrad. Stabil*. 2009, 94, 1076.
- [25] H. Nishida, M. Yamashita, Y. Andou, J.-M. Jeong, T. Endo, *Macromol. Mater. Eng*. 2005, 290, 848.
- [26] Y. Andou, M. Yasutake, H. Nishida, T. Endo, *J. Photopolym. Sci. Technol*. 2007, 20, 523.
- [27] M. Yasutake, Y. Andou, S. Hiki, H. Nishida, T. Endo, *J. Polym. Sci., Part A: Polym. Chem*. 2004, 42, 2621.
- [28] Y. Andou, M. Yasutake, J.-M. Jeong, M. Kaneko, H. Nishida, T. Endo, *J. Appl. Polym. Sci*. 2007, 103, 1879.
- [29] Y. Andou, M. Yasutake, J.-M. Jeong, H. Nishida, T. Endo, *Macromol. Chem. Physic*. 2005, 206,

1778.

- [30] M. Yasutake, Y. Andou, S. Hiki, H. Nishida, T. Endo, *Macromol. Chem. Physic.* 2004, 205 , 492.
- [31] M. Yasutake, S. Hiki, Y. Andou, H. Nishida, T. Endo, *Macromolecules* 2003, 36, 5974.
- [32] Y. Andou, J.-M. Jeong, S. Hiki, H. Nishida, T. Endo, *Macromolecules* 2009, 42, 768.
- [33] Y. Andou, J.-M. Jeong, H. Nishida, T. Endo, *Macromolecules* 2009, 42, 7930.
- [34] Y. Andou, J.-M. Jeong, H. Nishida, M. Kaneko, T. Endo, *Polym. J.* 2010, 42, 519.
- [35] A.-F. Mohd-Adnan, H. Nishida, Y. Shirai, *Polym. Degrad. Stabil.* 2008, 93, 1053.
- [36] J. Zhang, Y. Duan, H. Sato, H. Tsuji, I. Noda, S. Yan, Y. Ozaki, *Macromolecules* 2005, 38 , 8012.
- [37] N. Sgriccia, M. C. Hawley, M. Misra, *Compos., Part A: Appl S.* 2008, 39, 1632.
- [38] H. Yang, R. Yan, H. Chen, D. H. Lee, C. Zheng, *Fuel.* 2007, 86, 1781.
- [39] P. Pan, B. Zhu, W. Kai, T. Dong, Y. Inoue, *Macromolecules* 2008, 41, 4296.
- [40] P. Pan, W. Kai, B. Zhu, T. Dong, Y. Inoue, *Macromolecules* 2007, 40 , 6898.

Table 1. Vapor phase assisted surface polymerization of L,L-lactide on wood flour surfaces.

entry	wood flour <sup>a</sup>		time h	increment		$M_n$	$M_w$
	g	Catalyst mmol		g	wt% <sup>b</sup>		
1	0.20	0.025	3	0.16	80.0	300	1,300
2	0.24	0.030	6	0.31	129.2	500	1,600
3	0.22	0.028	9	0.86	390.9	800	2,200
4	0.20	0.025	15	1.25	625.0	1,600	5,100
5	0.25	0.031	24	1.65	660.0	4,700	12,100

Conditions: L,L-lactide 17.5 mmol, temperature 110°C.

<sup>a</sup> Sn(II)(Oct)<sub>2</sub> was supported, <sup>b</sup> against substrate weight.

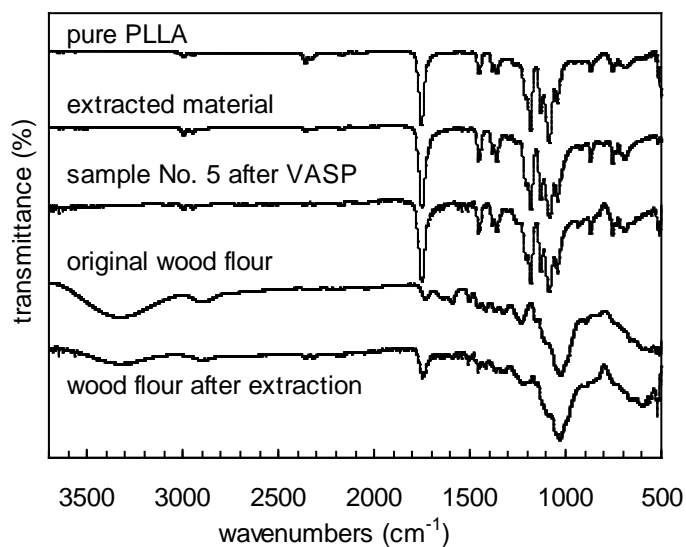


Figure 1. FT-IR spectra of original wood flour, sample No.5 after VASP of L,L-lactide, extracted material, residual wood flour after extraction, and pure PLLA.

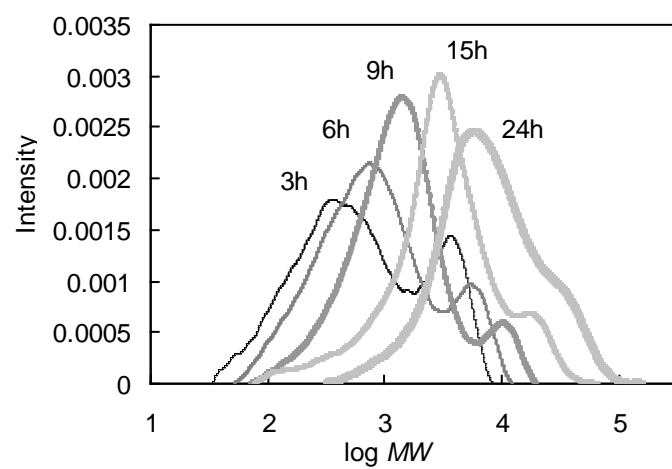


Figure 2. Changes in SEC profile of extracted materials from products after VASP.

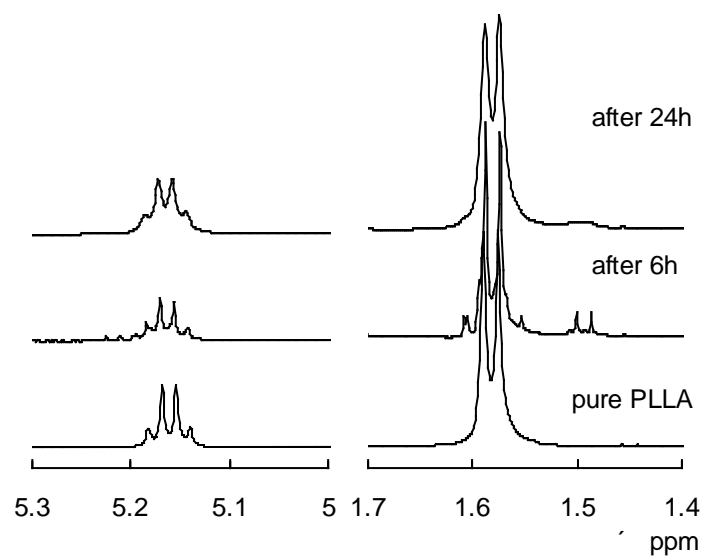


Figure 3.  $^1\text{H}$  NMR spectra of pure PLLA and extracted materials from products after 6 and 24h of VASP.

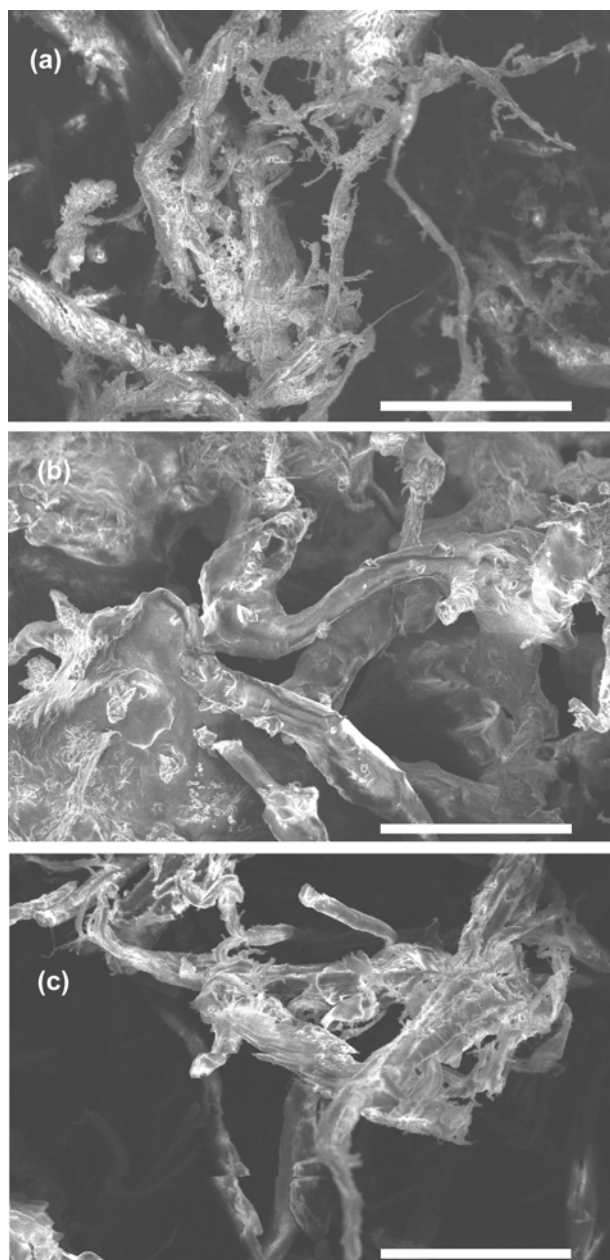


Figure 4. SEM micrographs of (a) original wood flour, (b) sample No. 5 prepared by VASP of L,L-lactide at 110°C for 24 h, and (c) residual substrates of sample No. 5 after 24h extraction using chloroform. Bar: 100  $\mu\text{m}$ .



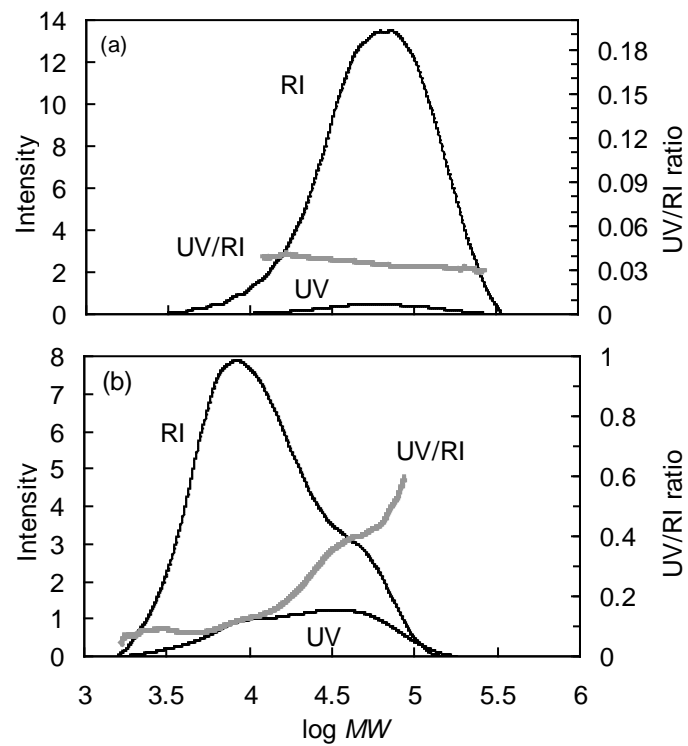


Figure 5. SEC profiles and UV/RI intensity ratios of (a) pure PLLA and (b) sample No. 5 after extraction treatment.

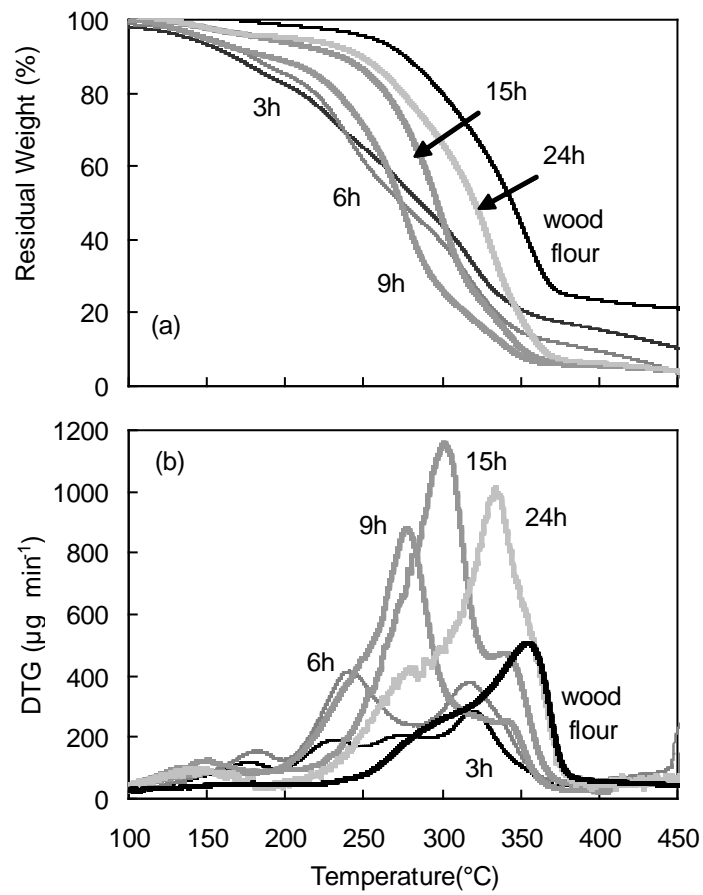


Figure 6. (a) TG and (b) DTG profiles of original wood flour and PLLA/wood flour composites prepared by VASP of LLA.

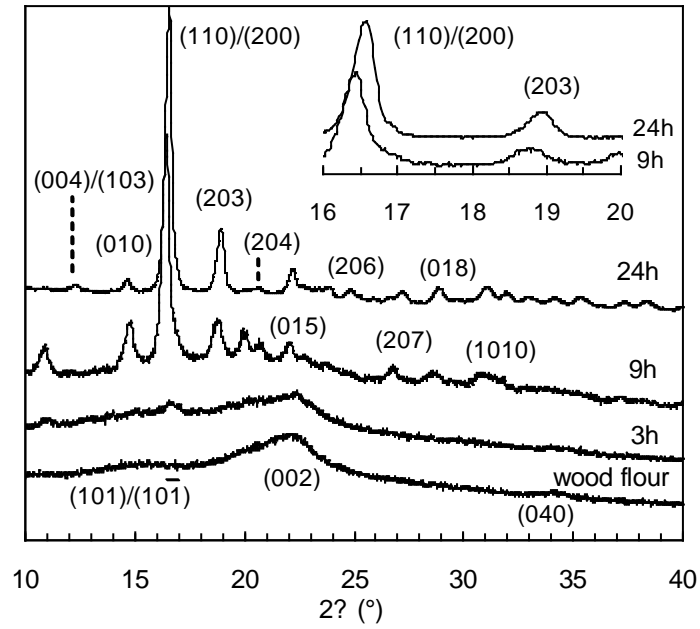


Figure 7. WAXD patterns of samples by VASP of L,L-lactide.

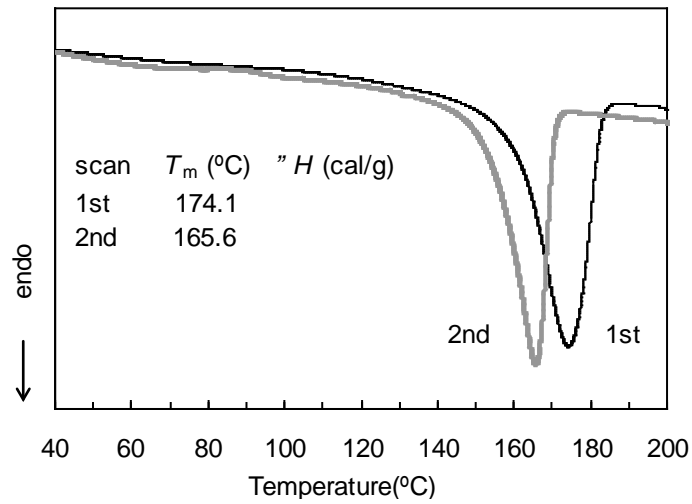


Figure 8. DSC curve of PLLA/Wood flour composite (sample No.5-24h).The heating and cooling rates are 10°C/min.

## Supporting Information

### Accumulation and Crystallization of Poly(lactic acid) Layers on Wood Flour Surface by Vapor-Phase Assisted Surface Polymerization

Donghee Kim,<sup>a</sup> Yoshito Andou,<sup>b</sup> Yoshihito Shirai,<sup>a,b</sup> Haruo Nishida<sup>b,\*</sup>

<sup>a</sup>*Graduate School of Life Science and Systems Engineering, Kyushu Institute of Technology, 2-4 Hibikino, Wakamatsu-ku, Kitakyushu, Fukuoka 808-0196, Japan*

<sup>b</sup>*Eco-Town Collaborative R&D Center for the Environment and Recycling, Kyushu Institute of Technology, 2-4 Hibikino, Wakamatsu-ku, Kitakyushu, Fukuoka 808-0196, Japan*

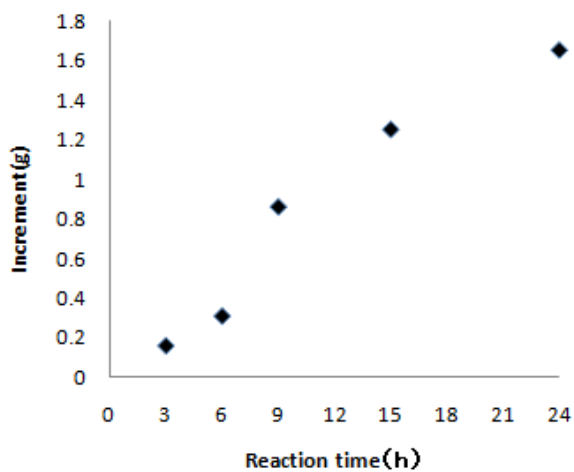


Figure S1. Changes in amount of accumulated PLLA with time of VASP.

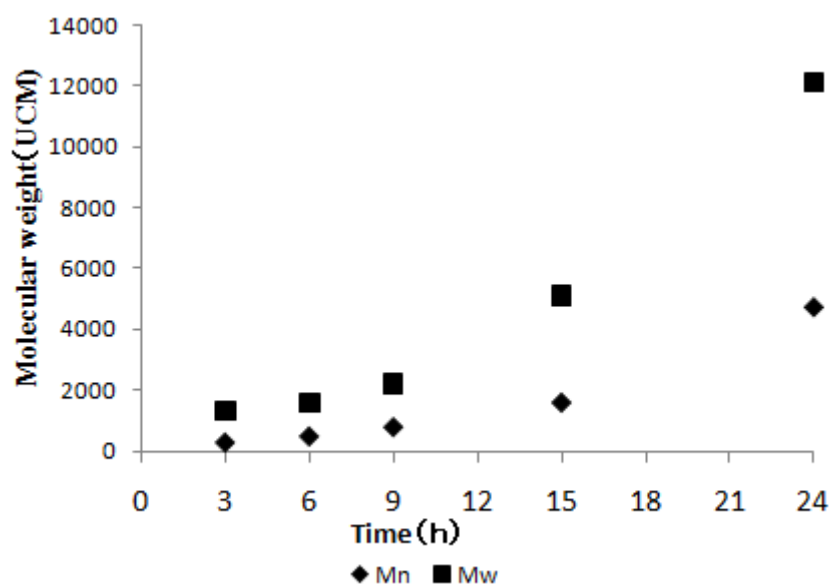


Figure S2. Changes in molecular weight of accumulated PLLA with time of VASP.

Table S1. UV/RI ratio of extracted samples after VASP.

entry	VASP time (h)	increment (wt%)	UV/RI ratio
S1-3	9	390.9	0.377
S1-4	15	625.0	0.216
S1-5	24	660.0	0.193
PLLA <sup>a</sup>	-	-	0.034

<sup>a</sup> Pure PLLA ( $M_n$  xxxxxx,  $M_w$  xxxxxx)

Table S2. Lattice spacing Crystal size derived from (110)/(200) and (203) reflections after VASP of L,L-lactide at different times.

entry	time (h)	plain (110)/(200) (nm)		plain (203) (nm)	
		<i>d</i> -space	crystal size	<i>d</i> -space	crystal size
S3-3	9	0.5385	23.63	0.4730	19.20
S3-5	24	0.5347	26.78	0.4681	22.39

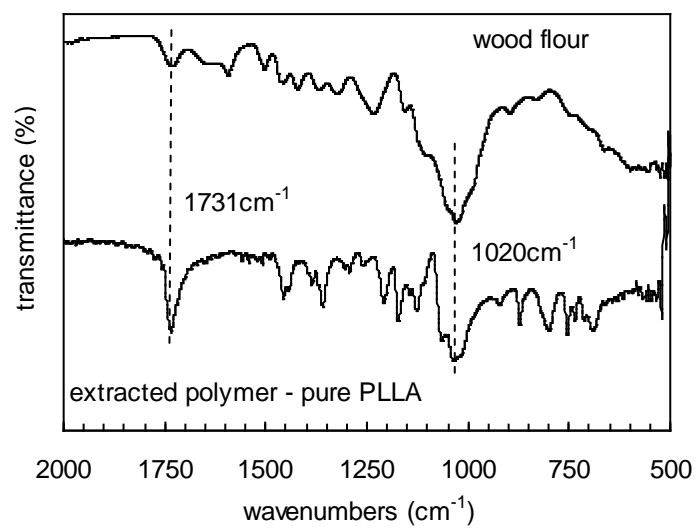


Figure S3. Difference spectrum between extracted sample No.5 and pure PLLA in comparison with wood flour.

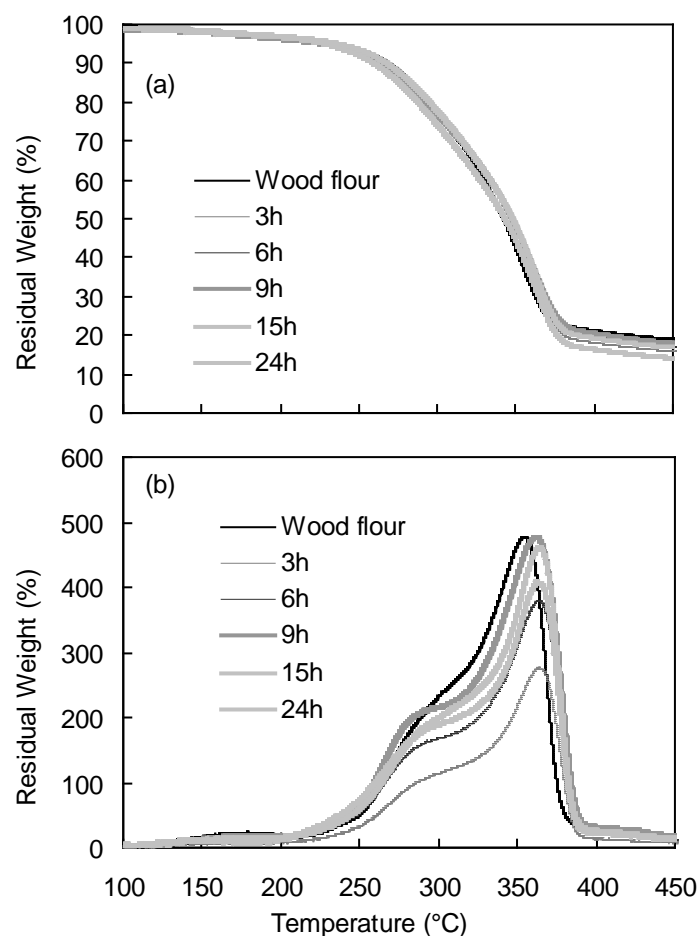


Figure S4. (a) TG and (b) DTG profiles of original wood flour and extraction treated residual wood flour samples No. 1-5.

<sup>1</sup> N. Chand, U. K. Dwivedi, *Wear*. 2006, 261,1057.

<sup>2</sup> A. K.Rana, A. Mandal, S. Bandyopadhyay, *Compos. Sci. Technol.* 2003, 63, 801.

<sup>3</sup> M.Brahmakumar, C. Pavithran, R. M. Pillai, *Compos. Sci. Technol.* 2005, 65, 563.

<sup>4</sup> P. A. Sreekumar, K. Joseph, G. Unnikrishnan, S. Thomas, *Compos. Sci. Technol.* 2007, 67, 453.

<sup>5</sup> M. Zampaloni, F. Pourboghrat, S. A. Yankovich, B. N. Rodgers, J. Moore, L. T. Drzal,

A. K. Mohanty, M. Misra, *Compos., Part A: Appl S.* 2007, 38, 1569.

<sup>6</sup> P. Yin, N. Nishina, Y. Kosakai, K. Yahiro, Y. Pakr, M. Okabe, *J. Ferment. Bioeng.* 1997, 84, 249.

<sup>7</sup> **H. R. Kricheldorf, I. Kreiser-Saunders, C. Boettcher, *Polymer* 1995, 36, 1253.**

<sup>8</sup> A. Takasu, Y. Narukawa, T. Hirabayashi, *J. Polym. Sci. Pol. Chem.* 2006, 44, 5247.

<sup>9</sup> K. W. Kim, S. I. Woo, *Macromol. Chem. Physic.* 2002, 203, 2245.

<sup>10</sup> F. Achmad, K. Yamane, S. Quan, T. Kokugan, *Chem. Eng. J.* 2009, 151, 342.

<sup>11</sup> G.-X.Chen, H.-S. Kim, E.-S. Kim, J.-S. Yoon, *Eur. Polym. J.* 2006, 42, 468.

<sup>12</sup> M. Ajioka, K. Enomoto, K. Suzuki, A. Yamaguchi, *J. Environ. Polym. Degrad.*, 1995, 3, 225.

<sup>13</sup> T. Kasuga, Y. Ota, M. Nogami, Y. Abe, *Biomaterials* 2001, 22, 19.

<sup>14</sup> M. S. Huda, L. T. Drzal, A. K. Mohanty, M. Misra, *Compos. Sci. Technol.* 2006, 66, 1813.

- <sup>15</sup> F. Chen, L. S. Liu, P. H. Cooke, K. B. Hicks, J. W. Zhang, *Ind. Eng. Chem. Res.* 2008, 47, 8667.
- <sup>16</sup> T. Nishino, K. Hirao, M. Kotera, *Compos., Part A: Appl S.* 2006, 37, 2269.
- <sup>17</sup> T.-M. Wu, C.-Y. Wu, *Polym. Degrad. Stabil.* 2006, 91, 2198.
- <sup>18</sup> L. Petersson, I. Kvien, K. Oksman, *Compos. Sci. Technol.* 2007, 67, 2535.
- <sup>19</sup> M. Noël, E. Fredon, E. Mougél, D. Masson, E. Masson, L. Delmotte, *Bioresource Technol.* 2009, 100, 4711.
- <sup>20</sup> L. T. Lim, R. Auras, M. Rubino, *Prog. Polym. Sci.* 2008, 33, 820.
- <sup>21</sup> R. Tokoro, D. M. Vu, K. Okubo, T. Tanaka, T. Fujii, T. Fujiura, *J. Mater. Sci.*, 2008, 43, 775–787.
- <sup>22</sup> F. Zhang, T. Endo, W. Qiu, L. Yang, T. Hirotsu, *J. Appl. Polym. Sci.*, 2002, 84, 1971–1980.
- <sup>23</sup> G. Grubbstrom, A. Holmgren, K. Oksman, *Compos., Part A: Appl S.* 2010, 41, 678.
- <sup>24</sup> M. Bengtsson, K. Oksman, *Compos., Sci. Technol.* 2006, 66, 2177.
- <sup>25</sup> M. Bengtsson, K. Oksman, *Compos., Part A: Appl S.* 2006, 37, 752.
- <sup>26</sup> H. Gao, Y.-M. Song, Q.-W. Wang, Z. Han, M.-L. Zhang, *J. Forestry Research*, 2008, 19, 315–318.
- <sup>27</sup> C.-S. Wu, *Polym. Degrad. Stabil.* 2009, 94, 1076.
- <sup>28</sup> M. Yasutake, S. Hiki, Y. Andou, H. Nishida, T. Endo, *Macromolecules* 2003, 36, 5974.
- <sup>29</sup> H. Nishida, M. Yamashita, Y. Andou, J.-M. Jeong, T. Endo, *Macromol. Mater. Eng.* 2005, 290, 848.
- <sup>30</sup> Y. Andou, M. Yasutake, H. Nishida, T. Endo, *J. Photopolym. Sci. Technol.* 2007, 20, 523.
- <sup>31</sup> M. Yasutake, Y. Andou, S. Hiki, H. Nishida, T. Endo, *J. Polym. Sci., Part A: Polym. Chem.* 2004, 42, 2621.
- <sup>32</sup> Y. Andou, M. Yasutake, J.-M. Jeong, M. Kaneko, H. Nishida, T. Endo, *J. Appl. Polym. Sci.* 2007, 103, 1879.
- <sup>33</sup> Y. Andou, M. Yasutake, J.-M. Jeong, H. Nishida, T. Endo, *Macromol. Chem. Physic.* 2005, 206, 1778.
- <sup>34</sup> M. Yasutake, Y. Andou, S. Hiki, H. Nishida, T. Endo, *Macromol. Chem. Physic.* 2004, 205, 492.
- <sup>35</sup> Y. Andou, J.-M. Jeong, S. Hiki, H. Nishida, T. Endo, *Macromolecules* 2009, 42, 768.
- <sup>36</sup> Y. Andou, J.-M. Jeong, H. Nishida, T. Endo, *Macromolecules* 2009, 42, 7930.
- <sup>37</sup> Y. Andou, J.-M. Jeong, H. Nishida, M. Kaneko, T. Endo, *Polym. J.* 2010, 42, 519.
- <sup>38</sup> H. Nishida, M. Yamashita, Y. Andou, J.-M. Jeong, T. Endo, *Macromol. Mater. Eng.* 2005, 290, 848.
- <sup>39</sup> N. Yasuda, Y. Wang, T. Tsukegi, Y. Shirai, H. Nishida, *Polym. Degrad. Stab.*, 2010, 95, 1238-1243.
- <sup>40</sup> H. R. Kricheldorf, I. Kreiser-Saunders, C. Boettcher, *Polymer* 1995, 36, 1253.
- <sup>41</sup> D. Garlotta, *J. Polym. Environ.*, 2001, 9, 63-84.
- <sup>42</sup> H. Nishida, M. Yamashita, Y. Andou, J.-M. Jeong, T. Endo, *Macromol. Mater. Eng.* 2005, 290, 848.
- <sup>43</sup> H. Nishida, M. Yamashita, Y. Andou, J.-M. Jeong, T. Endo, *Macromol. Mater. Eng.* 2005, 290, 848.
- <sup>44</sup> J. Zhang, Y. Duan, H. Sato, H. Tsuji, I. Noda, S. Yan, Y. Ozaki, *Macromolecules* 2005, 38, 8012.
- <sup>45</sup> N. Sgriccia, M. C. Hawley, M. Misra, *Compos., Part A: Appl S.* 2008, 39, 1632.
- <sup>46</sup> K. K. Pandey, *J. Appl. Polym. Sci.*, 1999, 71, 1969.
- <sup>47</sup> M. Yasutake, S. Hiki, Y. Andou, H. Nishida, T. Endo, *Macromolecules* 2003, 36, 5974.
- <sup>48</sup> M. Yasutake, Y. Andou, S. Hiki, H. Nishida, T. Endo, *J. Polym. Sci., Part A: Polym. Chem.* 2004, 42, 2621.
- <sup>49</sup> H. Yang, R. Yan, H. Chen, D. H. Lee, C. Zheng, *Fuel.* 2007, 86, 1781.
- <sup>50</sup> K. Wang, J. X. Jiang, F. Xu, R. C. Sun, *Polym. Degrad. Stab.*, 2009, 94, 1379.
- <sup>51</sup> P. Pan, B. Zhu, W. Kai, T. Dong, Y. Inoue, *Macromolecules* 2008, 41, 4296.
- <sup>52</sup> P. Pan, W. Kai, B. Zhu, T. Dong, Y. Inoue, *Macromolecules* 2007, 40, 6898.
- <sup>53</sup> J. Zhang, Y. Duan, H. Sato, H. Tsuji, I. Noda, S. Yan, Y. Ozaki, *Macromolecules* 2005, 38, 8012.
- <sup>54</sup> P. Pan, B. Zhu, W. Kai, T. Dong, Y. Inoue, *Macromolecules* 2008, 41, 4296.
- <sup>55</sup> P. Pan, W. Kai, B. Zhu, T. Dong, Y. Inoue, *Macromolecules* 2007, 40, 6898.



- 
- <sup>56</sup> J. Zhang, Y. Duan, H. Sato, H. Tsuji, I. Noda, S. Yan, Y. Ozaki, *Macromolecules* 2005, 38, 8012.
- <sup>57</sup> H. Tsuji, Y. Tezuka, S. K. Saha, M. Suzuki, S. Itsuno, *Polymer* 2005, 46, 4917.
- <sup>58</sup> P. Pan, W. Kai, B. Zhu, T. Dong, Y. Inoue, *Macromolecules* 2007, 40, 6898.